J. Cent. South Univ. (2014) 21: 2444−2453
DOI: 10.1007/s11771-014-2198-7

Springer

An automatic grid generation approach over free-form surface for architectural design

SU Liang(苏亮)[1, 2], ZHU Shun-lai(祝顺来)[1], XIAO Nan(肖南)[1, 2], GAO Bo-qing(高博青)[1, 2]

1. Department of Civil Engineering, Zhejiang University, Hangzhou 310058, China;
2. Zhejiang Provincial Key Laboratory of Space Structures, Hangzhou 310027, China

Abstract: An essential step for the realization of free-form surface structures is to create an efficient structural gird that satisfies not only the architectural aesthetics, but also the structural performance. Employing the main stress trajectories as the representation of force flows on a free-form surface, an automatic grid generation approach is proposed for the architectural design. The algorithm automatically plots the main stress trajectories on a 3D free-form surface, and adopts a modified advancing front meshing technique to generate the structural grid. Based on the proposed algorithm, an automatic grid generator named "St-Surmesh" is developed for the practical architectural design of free-form surface structure. The surface geometry of one of the Sun Valleys in Expo Axis for the Expo Shanghai 2010 is selected as a numerical example for validating the proposed approach. Comparative studies are performed to demonstrate how different structural grids affect the design of a free-form surface structure.

Key words: grid generation; free-form surface structure; architectural geometry; stress trajectory; advancing front meshing technique

1 Introduction

Since the first application of computer aided geometric design (CAGD) in architecture during the 1990s, the popularity of geometric modeling techniques has been constantly increasing [1]. Originated from aeronautic and car manufacturing industries, these design tools are gradually adopted and embedded into modern architectural design software. Over the past years, the emergence of parametric modeling and scripting techniques in architectural CAD applications has enabled a new level of sophistication in free-form designs, allowing architects and designers to create almost any shape imaginable. Complex free-form structure is one of the most striking trends in contemporary architecture. A large number of new building types with fanciful designs and eye-catching shapes have been successfully constructed, e.g. the British Museum Great Court Roof in London (Fig. 1(a)), the New Trade Fair in Milan (Fig. 1(b)) and the Sun-valley of Expo Axis in Shanghai (Fig. 1(c)).

Because the grid structure possesses a natural beauty and facilitates the geometric design created in digital models, many free-form surface geometries are normally triangularly meshed and covered by plane or curved glass panels, which is somewhat similar to traditional shell structures. As described by SCHLAICH and SCHOBER [2], these complex shell structures are regarded as free-form surface structures. However, with growing complexity in shape design, questions such as the realization of such free-form surfaces become increasingly challenging. Many examples can be found where a brilliant 3D-shape does not finally transfer into a real structure, because the relatively poor structural grid topologies make the architects have to give up their original architectural ideas.

Generally speaking, in order to practically realize these free-form surface structures and achieve an optimal solution, a continuous process of engineering from the original architectural idea to the structural assembly on site is necessary. The process basically consists of following steps:

1) Design of initial form (by architects);

2) Optimizing shape and all-over geometry (cooperation between architects and engineers);

3) Meshing (mainly by engineers and cooperation with architects for aesthetics);

4) Structural analysis and design of nodal connectors (by engineers);

5) Production and erection (by engineers and constructor).

While surface modeling is acceptable for producing initial geometry form at the early concept stage, the

Foundation item: Project(51378457) supported by the National Natural Science Foundation of China
Received date: 2013−01−21; **Accepted date:** 2013−07−13
Corresponding author: SU Liang, Associate Professor, PhD; Tel/Fax: +86−571−88208753; E-mail: suliang@zju.edu.cn

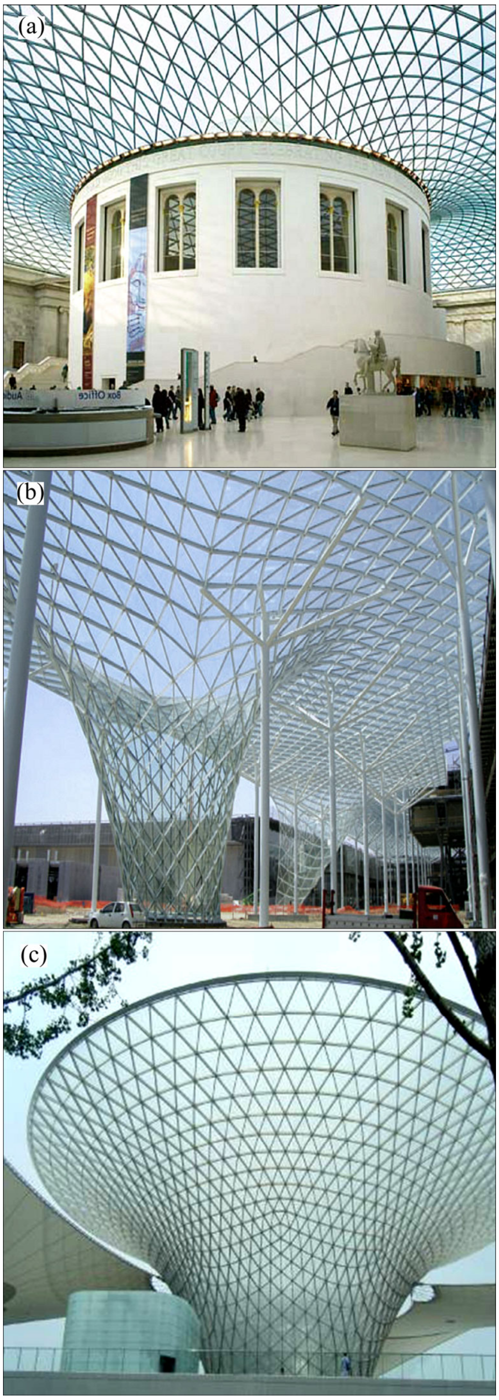

Fig. 1 Field applications of free-form surface structure: (a) British Museum Great Court Roof (London, England); (b) Vela-roof in Milan Trade Fair (Milan, Italia); (c) Sun-valley of Shanghai Expo Axis (Shanghai, China)

structural analysis and construction stages require a discretization of surface geometry into distinct elements that form an effective structural system. Among the above five steps from an engineering point of view, meshing of the architectural geometry (also known as grid generation over free-form geometry) turns out to be the essential step. The reason is that structural grid not only affects architectural aesthetics, but also determines the structural performance and complexity of construction assembly. However, despite of a good number of free-form structures that have been constructed successfully all over the world, their grid generations are still performed manually and case by case. Most of the grid generations are based on the expert experience of individual structural engineers. With the rapid increasing population of free-form surface structures, an automatic grid generation methodology that can create an efficient structural meshing over a given free-form surface, instead of relying upon manual generation by individual experience, will be attractive and necessary.

Based on the above engineering background, an automatic grid generation approach over free-form surface is proposed in this work. The approach adopts the concept of stress trajectory and FEM meshing technique.

2 Reviews on previous grid generation algorithms

Associated with the field constructions of previous free-form surface structures, substantial studies [2−9] have been carried out on the architectural meshing over free-form surfaces. Several grid generation algorithms have been proposed basically adopting the triangular element. These algorithms can be primarily divided into two main groups when dealing with the free-form geometry.

2.1 Grid generation algorithms based on expert experience

By far, the first group of grid generation algorithms relies on the expert experience of individual structural engineers. Generally, the auxiliary lines are firstly plotted to guide the direction orientation of main grids, and the deliberated meshing is then followed to form the final structural grid net. A typical example mentioned here is the Vela-roof in Milan Trade Fair [3]. The net geometry, i.e. grid topology, is generated in the introduction of three clusters of auxiliary lines. Both the position and orientation of these lines depend on the design experience of structural engineers. In other words, the acute sense of structural behavior is needed for drawing these auxiliary lines. As an example, the net geometry scheme of regions with steeper curvatures involves four steps as described in Ref. [3]. At the first two steps, two clusters of auxiliary lines were introduced to generate element corresponding to the existing mesh in the nearly non-curved regions. After that, the additional lines corresponding to the force flows were added to form the triangular net and then iterations were performed to obtain a final optimal grid meshing.

Another typical example is the MyZeil shopping mall [4], which is a part of the Palais Quartier in the very center of Frankfurt in Germany. To achieve a suitable net geometry which satisfies architectural aesthetics as well as structural performance, the structural engineers artificially define several lines of orientation as well as connection points for the vertical section. These lines and connection points were used as starting points or boundary conditions for the subsequent structural grid meshing.

To be noticed, in the present engineering practice, the plotting of auxiliary lines and grid generation process are mostly executed manually. Consequently, the efficiency and validity of such kind of grid generation algorithm are dependent on the individual intelligence of structural engineers. Two shortcomings will at least exist in their applications. Due to the complicated structural performance of 3D free-form structures, the auxiliary lines that are supposed to reflect the force flow are judged by the individual structural engineers approximately and in some cases even incorrectly. Furthermore, the steps of “optimizing shape and all-over geometry” and “meshing” as mentioned in “Introduction” should be accomplished with the tight cooperation between architects and engineers. As a result, the artificially meshing process can always be a terrible task due to the unavoidable frequent iteration works between architects and engineers during the preliminary design period of free-form surface structures.

2.2 Grid generation algorithms based on iterative optimization procedure

Here, we regard those methods that utilize iterative approach to acquire an optimal grid topology as the second meshing group. WINSLOW et al [5−6] presented an approach for the synthesis of single-layer grid structures, utilizing a multi-objective genetic algorithm to make a more informed selection of structural geometry. Unlike WINSLOW et al’s methods, LI and LU [7] proposed a different method that first generated grid manually and then iteratively adjusted the position and size of elements according to the analytical results of cable-net structural model. The validity and practicability of this method were also discussed for Sun Valleys of Shanghai EXPO Axis.

Despite of different iterative methods based on different models, initial mesh is the common prerequisite for this algorithm group and its mesh quality will affect the efficiency and convergence of the optimization algorithm directly. Again, to form an effective initial mesh needs a time-consuming processing of acquisition and elaboration of data and sometimes substantial manual works. For this reason, an automatic grid generation approach with the target of a good initial mesh will also be very useful before carrying out the iterative structural optimization analyses.

3 Overall procedures of proposed grid generation approach

The necessity of an automatic grid generation approach for the current field practice of free-form surface structure becomes very clear based on the above background analyses. The main objective of such automatic approach is to create a homogenous grid net geometry over the defined free-form surface, satisfying not only the architectural aesthetics but also the structural performance.

Based on the experience on free-form structures, SCHLAICH et al [2−3] illustrated the design principle for the visualization of the grid lines: the flow of grid lines should reflect the force flows on the free-form surface and the grid should be orientated according to the direction of these force flows. KNIPPERS and HELBIG [4] and POTTMAN [8] put forward the similar suggestion in their practical design works. Until now it has also become a common consensus that the net geometry should reflect or correspond to the force flows of free-form surface. Structural engineers believe that such meshing manner can generate a much better structural performance than other gird meshing manners although it has not been proven rigorous in theory [9].

Following the above principle, an automatic grid generation approach is proposed. The approach employs the main stress trajectories as the representative of force flow and a modified advancing front method as the automatic grid generation technique. One distinct feature of stress trajectories is that they indicate the local flow of stress and can give structural engineer sound feeling of the choice of grid [10]. For free-form surface shell, principal stresses are the components of the stress tensor that occur at each point of a continuum, which are purely axial. Consequently, their shear component equals zero. These components share the maximum and minimum stress values and ideally, if a grid is aligned along their directions, it can replace the continuum [10−12]. In order to realize the automatic gird generation and keep the main orientating direction of stress trajectories, the advancing front method is adopted as the grid generation algorithm in the view of its good performance to create the homogenous net geometry as well as to maintain the front-shape defined by stress trajectory curves [13].

The overall procedures of the proposed approach are depicted in Fig. 2. The procedure starts with the input of initial meshing information, including the free-form surface geometry, boundary condition and preferred structural element size, along with the stress analysis result of the shell structure with the same free-form geometry. The surface geometry to be meshed is typically represented by non-uniform rational B-splines (NURBS) [14] and assumed to remain fixed throughout the whole procedure. The user can specify the preferred element size range or define a size function to control the element size. Before starting the grid generation procedure, the auxiliary lines including the main principal stress trajectory curves and the boundary lines are generated to define directions of several clusters of primary rods. The next step is to form the triangular element over the free-form surface by the modified advancing front meshing technique. After above three steps, the grid optimization will be introduced to improve the quality of the grid meshing. The final stage involves producing the final grid geometry into output files, which are served as a data-model for structural analysis.

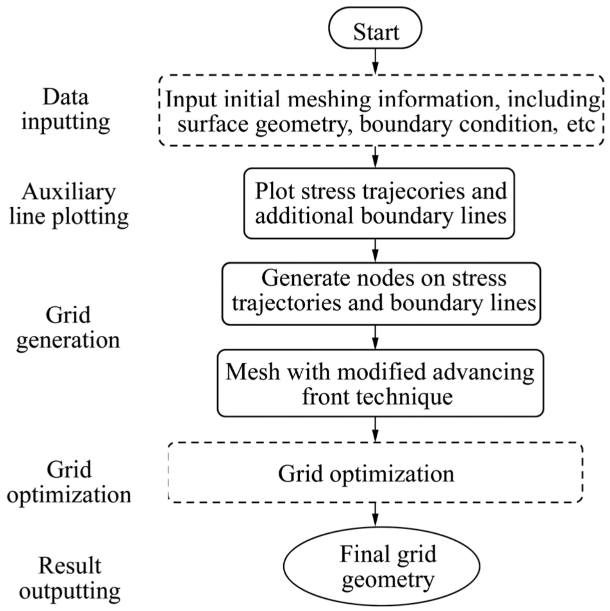

Fig. 2 Flowchart of procedures involved in proposed grid generation approach

4 Details of proposed grid generation approach

4.1 Pre-analysis of surface geometry

The proposed approach employs the main stress trajectory to represent the force flow of free-form surface. Thus the automatic net mesh can be realized by avoiding the artificial judgment of force flow based on the individual expert intelligence. Here, the stress trajectories are the curves whose tangents are the principal stress directions in stress field of continuums, such as 2D plates, 3D shells and beams. Consequently, a structural stress analysis on 3D shell with the same geometry of free-form surface is needed to gain the data of stress field as the prerequisite of stress trajectory plotting.

It should be pointed out that the precise structural stress analysis for continuum is not an easy work in the engineering practice, especially for the complex shell structure with free-form surface. Fortunately, the rapid developments of FEM theory and modern FEM analytical software make the stress analysis of continuum more convenient with the acceptable resource consumption. Furthermore, since the stress trajectories are just used to orientate the direction of force flow over the free-form surface, the precise and complex stress analyses are not needed in the proposed approach. By avoiding the elaborated efforts on determining the precise structural parameters, such as shell thickness and material properties, the stress pre-analysis of this section is in fact easy to be performed. Quite different from the detailed structural analysis, the pre-analysis process takes a simplified treatment as follows:

1) Import the surface geometry (which is always provided by the architects) to FEM analysis software.

2) Mesh surface geometry for FEM analysis of the shell structure. The mesh generated here is just used for FEM analysis. In order to improve the accuracy of the stress trajectories, the element size would not exceed one half of the dimension of element in final net geometry. There is no limit to the finite element form and either triangular or quadrilateral net can be adopted.

3) Perform computation and analysis. Carry out a 3D finite element analysis of the surface geometry under specified loading case and support condition. The surface geometry described above is represented by anisotropic continuum shell finite elements in this process. As stress trajectories are determined by the load, support and geometry, the analysis model should also coincide with these actual conditions.

4) Export result files. Currently, ready-made procedure that draws stress trajectory automatically is rarely available in the mainstream finite element software. Thus, the mesh data file and the principal stress data file of FEM analysis are needed to portray the stress trajectory curves in the proposed approach.

4.2 Plotting of stress trajectory curves

In the field of photoelasticity, several techniques [15] have been developed for plotting principal stress trajectories to investigate stress state in two-dimensional stress field. Researches on numerical methods have also been ongoing for the similar problem. For instance, JO et al [16] described an algorithm to plot the principal stress trajectories using the constant strain triangular element direction function. Quite recently, a finite-element approach with the use of Hermitian splines as basic functions for plotting stress trajectories was proposed by MARCHUK and KHOMYAK [17].

For the problem of two-dimensional stress field, a stress field can be represented as a vector field using the notions of two principal stresses [18]. The values and the directions of two mutually perpendicular principal stresses can be calculated by Eq. (1) and Eq. (2) respectively:

$$\sigma_{1,2}=\frac{\sigma_x+\sigma_y}{2}\pm\sqrt{\left(\frac{\sigma_x-\sigma_y}{2}\right)^2+\tau_{xy}{}^2} \tag{1}$$

$$\tan(2\alpha)=2\tau_{xy}\frac{1}{\sigma_x-\sigma_y} \tag{2}$$

where σ_x, σ_y and τ_{xy} are the normal and shear stresses in the corresponding x-y coordinate. α represents the angle between x axis and the direction of the maximum (first) principal stress σ_1, and $0°\le\alpha\le 90°$. The direction of the second principal stress σ_2 is perpendicular to that of σ_1.

According to Eqs. (1) and (2), the vector field of principal stresses can be expressed in the form of a pair of crossed arrows turned by an angle α from x axis, which indicates the direction of tension-compression at the corresponding point. Assuming that the stress field in a domain is known, or in other words, two mutually perpendicular vector fields of principal stresses are known, it is not a difficult job to draw two families of the stress trajectories [16−17]. Figure 3 conceptually illustrates the plotting of the stress trajectories S_1 and S_2 from the given vector fields both in the rectangle and triangle unit cells. Here, S_1 represents the contour of maximum (first) principal stress trajectory and S_2 represents the minimum principal stress trajectory.

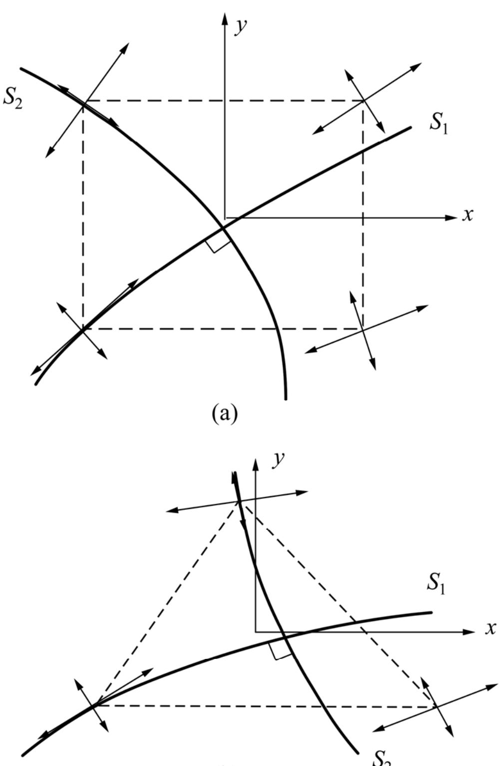

Fig. 3 Plotting of two families of stress trajectories in plane system: (a) Unit rectangle of regular mesh; (b) Unit triangle of regular mesh

Unfortunately, with respect to the problem of three-dimensional stress field, less research has been conducted for portraying principal stress trajectories and few literatures were published on this subject. Thus, in order to realize the automatic plotting of stress trajectories over the free-form surface, an approximation algorithm is proposed in the work, which transforms 3D problem to a simpler work of plotting stress trajectories in 2D plane system.

The algorithm implements a simple stepwise manner to plot the stress trajectories throughout the underlying FEM mesh faces. After mapping stress data onto each FEM planar element, the user can pick one pre-specified element as starting cell for each principal stress trajectory. The first trajectory segment can thus be generated on this 2D pre-specified planer element. Following the direction of principal stress vector field, the next stress trajectory segment will then be plotted in the adjacent element. The plotting process is repeated until meeting one of the terminating conditions. The process of algorithm is presented in Fig. 4. Some major steps are explained in detail as follows.

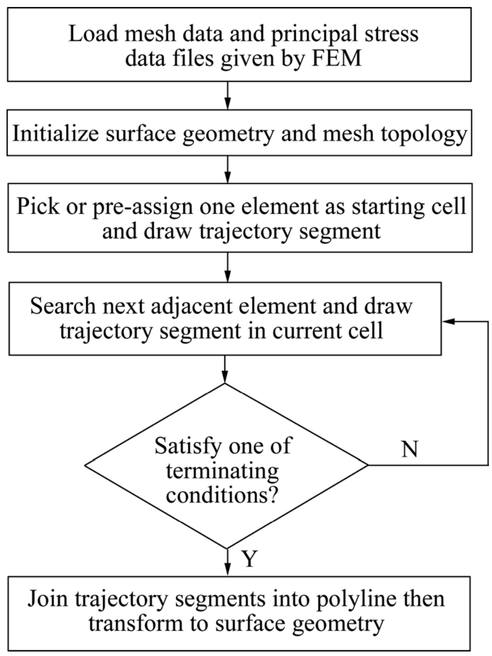

Fig. 4 Algorithm for plotting stress trajectory over 3D free-form surface

1) Basic requirements

The required data for the proposed algorithm include surface geometry model, FEM mesh data and principal stress vector data, which can be obtained in the FEM pre-analysis stage. For each element, a continuum stress vector field is constructed through linear interpolation method, by using the stress data at the element nodes. Therefore, it is assumed that the stress field in the surface domain is known.

2) Choosing one element as starting element cell

So far, the described procedure provides two available ways for choosing the starting elements: one is pre-assigning the spacing distance L between any pair of adjacent final stress trajectories and thus the starting element of each stress trajectory can be picked up automatically; the other way is picking up the starting element interactively in a manual way.

3) Drawing stress trajectory segments

Before paying attention to drawing stress trajectory segment on each element, two necessary notes should be pointed out: (1) the proposed algorithm is suitable for both the FEM triangular and quadrilateral elements and (2) only the maximum or minimum principal stress in element plane is considered to plot the stress trajectory segment since the out plane stress of 3D shell is small enough to be ignored.

For each element, a local coordinate system with the origin located in the center of the element is introduced for calculation convenience, as shown in Fig. 3. Since the stress field of the element is pre-known, the trajectory segment can be generated by employing the method suggested by MARCHUK and KHOMYAK [17] for 2D plane. For each stress trajectory segment, its intersection points to element borders need to be identified and their positions in the global coordinate should be calculated to determine the element locations of the next stress trajectory segments. The stress trajectory segment on the starting cell originates at the centroid of element, while other segments take the end point of previous segment as the starting point (Fig. 5). The basic procedure to plot all the stress trajectory segments along with the target stress trajectory curve is illustrated as follows.

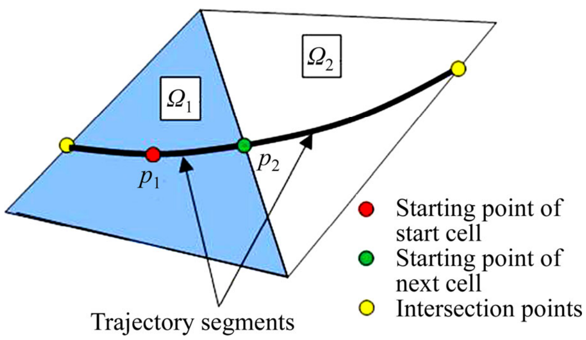

Fig. 5 Draw stress trajectory segments in a stepwise manner

As shown in Fig. 5, Ω_1 and Ω_2 are two adjacent elements and P_2 is the intersection point between the former trajectory segment and the element border. Ω_1 is assumed to be the starting cell and the first segment is drawn through the center of the element (P_1). The coordinates of the end point of the segment are calculated and then a search algorithm based on local topology information along with automated phase-shifting method is executed to find out the next element Ω_2. Starting from P_2, a new segment is drawn following direction of the principal stress field of Ω_2. The above procedure is repeated to plot all the stress trajectory segments along with the target stress trajectory until one of the following terminating conditions is satisfied:

(1) The directions of maximum or minimum principal stress vector in two adjacent elements change sharply in a single step.

(2) The current trajectory segment meets surface boundary or reaches outside the target domain.

(3) The current trajectory segment reaches an element on which corresponding trajectory segment has been generated.

4) Transforming stress trajectory segments to surface geometry.

Note that the stress trajectory segments generated above are not the curves lying on the original free-form surface geometry but polyline on the underlying FEM mesh, as shown in Fig. 6. In order to solve this problem, one can transform the trajectory segments to basic surface by means of the parameter domain. In this work, the surface geometry is represented in the form of NURBS and the parameterization coordinate (u,v) can be expressed as [14]

$$(x, y, z)^{\mathrm{T}} = \boldsymbol{r}(u, v) \tag{3}$$

Using Eq. (3), it is convenient to map all segments into parametric space (u,v) and join them to a continuous polyline. After that, a complete trajectory curve which lies on the original free-form surface will be obtained simply by transforming the multi-segment curves back to the original real space (x, y, z).

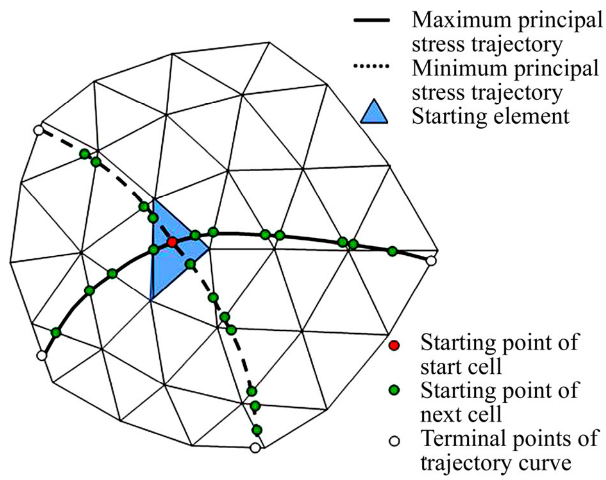

Fig. 6 Graph of stress trajectory polyline on underlying mesh

Experiments indicate that the above described algorithm is compact and of easy implementation to obtain the stress trajectory curves on 3D free-form surface from the pre-known stress field. Evenly spaced curves can be achieved via elaborately selecting starting elements. Before starting element generation, smoothing algorithm [19] can be further used to all trajectory curves to expect a much better result.

4.3 Grid generation

With the rapid development of FEM theory and its engineering application, great research efforts have been done on the FEM mesh generation over arbitrary two-dimensional or three-dimensional geometry in the past 40 years [13, 20−22]. Quite a lot of manual, semi-automatic, and automatic mesh generation methods can be found in research literatures and FEM softwares. These methods can be used as the references for the grid generation of free-form surface structure. Of course, due to the different objectives of grid generation, the methods in FEM field should be modified when their implements are diverted to the grid generation of free-form surface structure. In this work, taking into account its efficiency and performance, the advancing front meshing technique of FEM is selected and modified to be the automatic grid generation algorithm on the free-form surface.

Analogous to the tradition advancing front meshing technique of FEM [13, 20−22], the modified algorithm for grid generation over free-form surface also consists of four sub-problems: initial point calculation, edge division, surface meshing and optimization process. Depending on the 3D free-form surface geometry, the whole meshing procedure of this work is sketched as follows.

Modified advancing front algorithm for grid generation:

```
Load surface geometry and set element size field
Detect initial points
Divide stress trajectory curves and surface boundary
Initialize starting front
While the front is not empty
    Process the front for element generation;
    Store element data;
    Update front;
Mesh optimization
```

The algorithm begins with the calculation of initial points and then discretizes stress trajectory curves and boundary curves of surface geometry to form the starting front. The most time-consuming process is to advance the meshing front and to generate the new elements towards the interior of the unmeshed domain. When the meshing front is detected to be empty, the initial meshing work is finished and the mesh optimization will be executed to obtain a much better grid layout result. The above generation procedure is similar to that of the traditional advancing front meshing technique, and the algorithm proposed by LEE and HOBBS [22] is adopted as the basic reference to build the meshing algorithm of this work. Of course, in order to achieve the final grid objective of free-form surface structures, several special aspects of the grid generation procedure should be modified as follows when comparing with the traditional advancing front meshing algorithm.

4.3.1 Defining element size field

Definition of the mesh size field is the first step for grid generation. In FEM field, the mesh size field is determined by the accuracy requirement of analytical problem and the denser element grid always means more accurate analytical result and more computation effort. Quite different from the grid meshing work of FEM, the grid rods of free-form surface structures should be assigned a rational uniform length to achieve an optimal structural performance and a good mapping on the original surface geometry. The grid density thus is approximately constant all over the free-form surface. Considering the field practice of free-form surface structures, the average length of the rod element is set to be 2.0 m and its range changes from 1.5 m to 3.0 m as adopted in the numerical example of the work.

4.3.2 Discretizing curves

Note that a series of stress trajectory curves have been generated on surface in the foregoing steps, and they are sent into the mesh generator along with the surface geometry model. Different from the traditional advancing front meshing technique where only boundary curves are discretized, these stress trajectory curves should also be discretized to form their own starting front to orientate the grid directions over the free-form surface. Furthermore, when the stress trajectory curve intersects with the boundary curve, their intersection point should also be a discretization point of boundary curves, that is to say, the original one boundary curve is divided into two boundary curves by the intersection point during the discretization procedure. In the implementation of this work, both the stress trajectory and boundary curves are modeled by the NURBS and the method proposed by LEE and HOBBS [22] is adopted to discretize these curves according to the pre-defined size field.

4.3.3 Processing front for element generation

Once all the stress trajectory curves and boundary curves are discretized, these segments will be initialized as the starting front and advanced to the unmeshed domain to generate the grid layout of free-form surface. In order to realize the orientating function of the stress trajectory curves, the priority ratio ρ_i is set to each segment on the front and it can be calculated as follows:

$$\rho_i = v_i + l_i + n \times R \tag{5}$$

where v_i is an index associated with the type of each front segment. For the segments advanced from the stress trajectory curves, the value of v_i equals zero, and for the segments advanced from the boundary curves, the value of v_i equals 10. l_i is the length of each front segment. And n represents the distance between the starting front and the currently calculated front segment, which is determined by the generation layer number of the calculated front segment from the starting front. R is an amplification factor which is set to be 10.

In the advancing procedure, the front segment with the minimum value of ρ_i will be selected to be the base-segment. And the next new element will be generated from the base-segment either by producing a new node or by connecting it to an existing front node, which is depended on the quality of the newly generated element. After a new element is formed, its data will be stored and the generation front will be updated for the creation of the next new element. To be noticed, in the calculating of the priority ratio ρ_i, the value of v_i determines that the segment advanced from stress trajectory curves owns a priority to be the base-segment compared with the other segments and the value of $n\times R$ means that the generation procedure will be advanced layer by layer. These two measures ensure that the grid stem parallel to the direction of pre-defined stress trajectory curves will be generated preferentially during the advancing front procedure. As a result, the net geometry created by this manner will achieve the original objective to reflect the force flows of the free-form surface.

4.4 Grid optimization

After the initial meshing works, a few locally distorted elements may still emerge despite of the overall homogeneous grid layout, particularly when the free-form surface varies sharply. For these elements, grid optimization algorithm is needed to adjust their meshing qualities. Here, the original grid segments lying on the stress trajectory curves will be fixed during the optimization process due to their original function of direction orientation for main grid flows. In the implement of this work, the general Laplacian optimization method is adopted as the main grid optimization algorithm. A function expressed by Eq. (6) is used to evaluate the quality of each generated triangular element:

$$E(T)=\frac{\sqrt{3}}{36}\frac{\left(\sum_i l_i\right)^2}{A}+\sum_i\left(\frac{l_i}{h}+\frac{h}{l_i}-2\right) \quad (6)$$

where l_i is the edge length, i=1, ⋯, 3; A and h are the area and height of triangular element, respectively. With the definition, the equilateral triangle has a quality ratio $E(T)$ that equals 1 and for degenerated triangle the value of $E(T)$ will tend to be infinity. The objective of the gird optimization is to decrease the total quality functional value which is the sum of all the elements.

5 Automatic grid generator and numerical example

Following the above described grid generation procedure, an automatic grid generator named as "St-Surmesh" is developed for the practical architectural design of free-form surface structures. The generation program is built from the software development platform of Open CASCADE which is an open-source development platform for 3D CAD, CAM, CAE, etc. The C++ programming language is adopted in "St-Surmesh" combined with the utilization of microsoft foundation classes (MFC).

As a numerical example of 3D free-form structures, the surface geometry of one of the Sun Valleys in Expo Axis for the Expo Shanghai 2010 is selected to be meshed using the proposed grid generation approach. Figure 7 illustrates the basic geometry of the target surface and its shape likes a trumpet flower. The structural height is 41 m. The top and bottom of the structure are both ellipses and their diameters are 90 m, 70 m and 21 m, 15 m, respectively. The structure is restrained at the bottom ellipse against the translation in all the directions.

In the pre-analysis procedure, the surface geometry is imported into the FEM software of ANSYS and modeled as a shell structure. Only the self-weight and wind load of the structure (Fig. 7(b)) are considered in stress calculation. With the analytical result of FEM, five main stress trajectory curves are plotted on the surface based on the output of pre-analysis. As illustrated in Fig. 8,

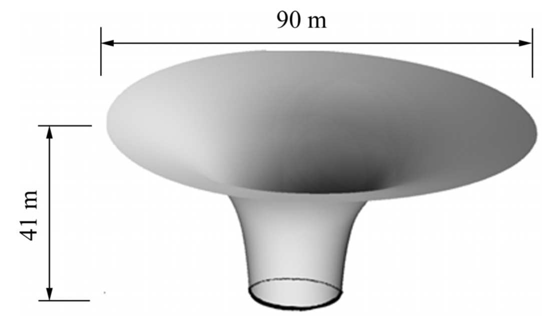

(a)

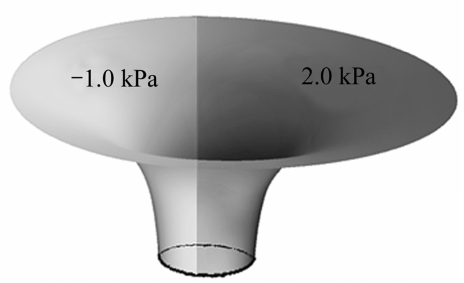

(b)

Fig. 7 Example free-form surface analyzed: (a) Example surface model of Sun Valley; (b) Wind load case

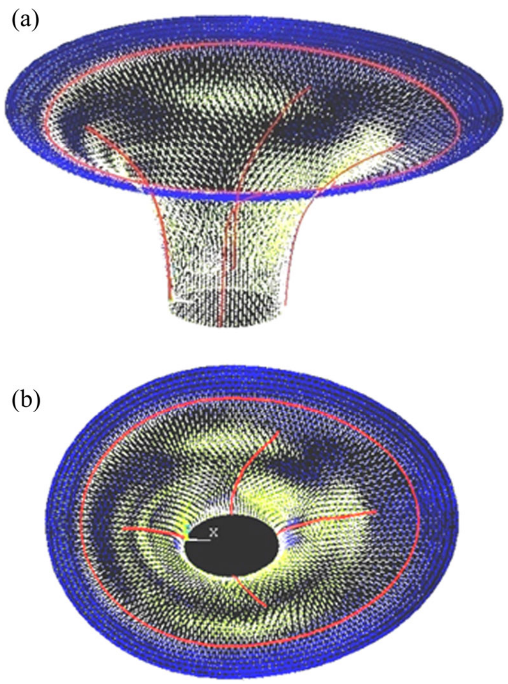

Fig. 8 Stress trajectory curves plotted over free-form surface: (a) Side view; (b) Top view

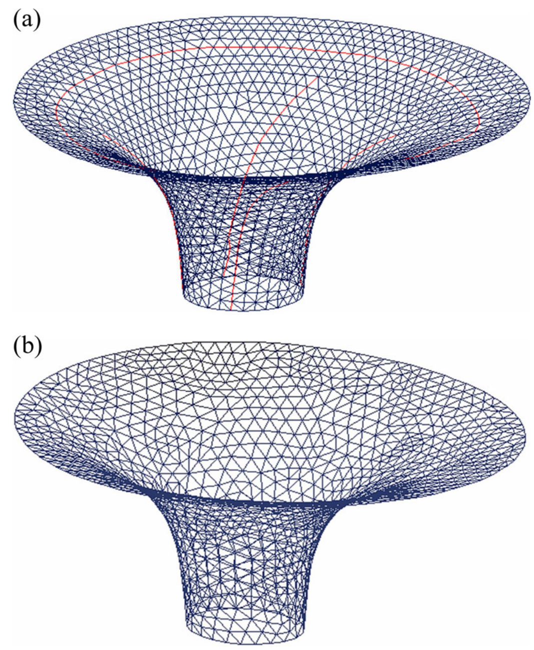

Fig. 9 Grid layout results of free-form surface of example geometry: (a) Generated by “St-Surmesh”; (b) Generated by “Gmsh”

at the lower part of the structure, the main force flows are vertical; while on the upper part, the main force flows are horizontal. The space distance L between each stress trajectory curve is set to be 15−20 m. Experiments show that, for most cases, the optimal grid layout will be created when the space distance L is about 8−10 times of the element size.

Given the element grid size of 1.5−3.0 m, the grid layout on the above free-form surface is created by the “St-Surmesh” automatic grid generator. As shown in Fig. 9(a), the main grid flows of the final meshing result are concordant with their orientation directions that are pre-defined by the stress trajectory curves as expected. The result means that the proposed grid generation algorithm can achieve its primary objective. As a comparison, the same surface is also meshed using the traditional FEM meshing technique and one case of the meshing result created by the grid generator of “Gmsh” [23] is illustrated in Fig. 9(b). By comparison of two models, it can be found that the gird layout tends to be more neat and reasonable in the view of the architectural aesthetics when its main grid flows are orientated by the stress trajectory curves. Also it can be found that the gird layout created by “St-Surmesh” generator is very close to that of the real engineering application of Sun-valley of Shanghai Expo Axis and its image is illustrated in Fig. 1(c).

In order to have a primary understanding on the meshed structures, the above two structural models, whose gird layout is created by the automatic generators of “St-Surmesh” and “Gmsh”, respectively, are analyzed and the results are given in Table 1. NE and NP are the element number and node number corresponding to different models. It can be noticed that NE and NP of two models are close to each other due to the similar setting of the element size. N_{max} and N_{min} are the maximum and minimum axial forces and M_{max} is the maximum bending moment of the structural gird members. Adopting the fully stressed design principle, the structural sections of grid members are designed and the whole steel amounts are calculated. The rectangular section is adopted for structural members and their width directions are perpendicular to the free-form surface. As listed in Table 1, the range of section width of structural grid members is set to be 40−100 mm with increasing size at 5 mm step by step and the range of section height

Table 1 Preliminary design comparison of two grid structures

Structural model	Element number (NE)	Node number (NP)	N_{max}/kN	N_{min}/kN	M_{max}/(kN·m)	Section width/ mm	Section height/ mm	Steel amount/ kg
Gmesh	4790	1692	1420.9	−1900.5	−406.6	40−100	120−300	265×10^3
St-Surmsh	4816	1704	1483.8	−1670.6	−394.1	40−100	120−300	218×10^3

is 120−300 mm with increasing size at 15 mm accordingly. It can be seen from the statistics results that steel amount of the structural model created by “St-Surmesh” is about 20% less than that of the other. This result indicates that a more efficient structural performance can be achieved when the structural grid layout is created by the described method.

6 Conclusion and future research

An automatic grid generation approach over free-form surface for architectural design has been proposed. The primary objective of the approach is to automatically generate the grid mesh that satisfies not only the architectural aesthetics but also the structural performance for free-form surface structures. The approach employs the main stress trajectory as the representative of force flow to orientate the main gird directions and adopts a modified advancing front meshing technique for the grid generation. How to plot the main stress trajectory automatically over 3D free-form surface is introduced in detail. And the differences between the modified advancing front meshing technique and the traditional one are also presented. Based on the above two algorithms, the authors attempt to develop an automatic grid generator named “St-Surmesh” for the practical architectural design of free-form surface structure.

As a numerical example of 3D free-form structures, the surface geometry of one of the Sun-valleys in Expo Axis for the Expo Shanghai 2010 is selected to be meshed using the proposed approach. The mesh result shows that the grid generator can create a satisfied grid layout for 3D free-form structures. Not only the main grid flows reflect the direction orientated by the main stress trajectories as expected, but also the meshing quality is quite high with the homogeneous element size and the good architectural aesthetics. One case of grid mesh over the same surface geometry is also created by the traditional meshing technique as a comparison. Further comparison analysis shows that much better structural performance can be reached when the grid layout is generated by the proposed approach.

It should be pointed that, although engineers agree that the main grid direction of free-form structure should reflect its force flow in the present field practice and the numerical example also has shown that such grid manner gains a better structural performance, the rigorous theoretical investigations will still need to prove such engineering point of view. With the meshing generator of “St-Surmesh”, it will be not a difficult task to do research on this subject for the more future application of free-form surface structures in modern society.

References

[1] LACHAUER L, KOTNIK T. Geometry of structural form [C]// Advances of Architectural Geometry 2010. Vienna, 2010: 193−203.

[2] SCHLAICH J, SCHOBER H. Design principles of glass roofs [C]// Proceedings of International Conference on Lightweight Structures in Civil Engineering. Warsaw, 2002: 815−827.

[3] SCHLAICH J, SCHOBER H, KURSCHNER K. New trade fair in Milan-grid topology and structural behavior of a free-formed glass-covered surface [J]. International Journal of Space Structures, 2005, 20: 1−14.

[4] KNIPPERS J, HELBIG T. The Frankfurt Zeil grid shell [C]// IASS Symposium. Valencia, Spain, 2009.

[5] WINSLOW P, PELLEGRINO S, SHARMA S B. Multi-objective optimization of free-form grid structures [J]. Structural and Multidisciplinary Optimization, 2010, 40: 257−269.

[6] WINSLOW P. Synthesis and optimization of free-form grid structures, [D]. University of Cambridge, 2009.

[7] LI C M, LU D. Study of intelligent layout design of single-layer lattice shell of free form surface [J] China Civil Engineering Journal. 2011, 44: 1−7. (In Chinese)

[8] POTTMAN H. Geometry and new and future spatial patterns [J]. Architectural Design, 2009, 79: 60−65.

[9] WILLIAMS C J K. The analytic and numerical definition of the geometry of the British museum great court roof [C]// Mathematics & Design. Geelong, Australia, 2001: 434−440.

[10] THAMM F. The role of the stress trajectories as an aid in the choice of the suitable shape of load-bearing structural element of engines and structure [J]. Periodica Polytechnic Mechanical Engineering, 2000, 44: 171−183.

[11] MICHALATOS P, KAIJIMA S. Design in a non-homogeneous and anisotropic space [C]// IASS Symposium. Venice, Italy, 2007.

[12] KELLY D W, TOSH M W. Interpreting load paths and stress trajectories in elasticity [J]. Engineering Computations, 2000, 17: 117−135.

[13] GEORGE P L, SEVENO E. The advancing-front mesh generation method revisited [J]. International Journal of Numerical Methods in Engineering, 1994, 37: 3605−3619.

[14] PIEGL L, TILLER W. The nurbs book [M]. Berlin, Springer-Verlag, 1997.

[15] DALLY J W, RILEY W F. Experimental stress analysis, third ed [M]. New York, McGraw-Hill, 1991.

[16] JO M, TAGUCHI M, SUZUKI H. Automatic plotting of principal stress trajectories by direction function contouring [J]. 2000, 68: 385−390. (In Japanese)

[17] MARCHUK M V, KHOMYAK M M. Hermitian splines as basic functions of the finite-element method for plotting stress trajectories [J]. Journal of Mathematical Sciences, 2010, 168: 673−687.

[18] TIMOSHENKO S P, GOODIER J N. Theory of elasticity [M]. McGraw-Hill, New York, 1970.

[19] SAPIDISA N, FARIN G. Automatic fairing algorithm for B-spline curves [J]. Computer-Aided Design, 1990, 22: 121−129.

[20] LO S H. Finite element mesh generation and adaptive meshing [J]. Progress in Structural Engineering and Materials, 2002, 4: 381−399.

[21] LAN T S, LO S H. Finite element mesh generation over analytical curved surfaces [J]. Computers and Structures, 1996, 59: 301−309.

[22] LEE C K, HOBBS R E. Automatic adaptive finite element mesh generation over rational B-spline surfaces [J]. Computers and Structures, 1998, 69: 577−608.

[23] GEUZAINE C, REMACLE J F. Gmsh: A three-dimensional finite element mesh generator with built-in pre- and post-processing facilities [J]. International Journal for Numerical Methods in Engineering, 2009, 0: 1−24.

(Edited by YANG Bing)